Blood flow–metabolic relationships are dependent on tumour size in non-small cell lung cancer: a study using quantitative contrast-enhanced computer tomography and positron emission tomography

K. A. Miles[1], M. R. Griffiths[2], C. J. Keith[3]

[1] Division of Clinical and Laboratory Sciences, Brighton & Sussex Medical School, University of Sussex, Brighton, BN7 3PB, UK
[2] Queensland University of Technology, Gardens Point Brisbane, Brisbane, Australia
[3] The Wesley Research Institute, Chasely Street, Brisbane, Australia

Received: 12 July 2005 / Accepted: 2 August 2005 / Published online: 23 September 2005

Abstract. *Purpose:* The purpose of this study was to undertake dual assessment of tumour blood flow and glucose metabolism in non-small cell lung cancer (NSCLC) using contrast-enhanced computed tomography (CE-CT) and ^{18}F-fluorodeoxyglucose positron emission tomography (FDG-PET) in order to assess how the relationships between these parameters vary with tumour size and stage.
Methods: Tumour blood flow and glucose metabolism were assessed in 18 NSCLCs using quantitative CE-CT and FDG-PET respectively. Contrast enhancement and FDG uptake were both normalised to injected dose and patient weight to yield correspondingly the standardised perfusion value (SPV) and standardised uptake value (SUV). Tumour area was measured from conventional CT images.
Results: The ratio of SUV to SVP and the metabolic–flow difference (SUV–SVP) correlated with tumour size (r=0.56, p=0.015 and r=0.60 and p=0.008 respectively). A metabolic–flow difference of greater than 4 was more common amongst tumours of stages III and IV (odds ratio 10.5; 95% confidence limits 0.24–32.1). A significant correlation between SUV and SPV was found only for tumours smaller than 4.5 cm^2 (r=0.85, p=0.03).
Conclusion: Blood flow–metabolic relationships are not consistent in NSCLC but depend upon tumour size and stage. Quantitative CE-CT as an adjunct to an FDG study undertaken using integrated PET-CT offers an efficient way to augment the assessment of tumour biology with possible future application as part of clinical care.

K. A. Miles (✉)
Division of Clinical and Laboratory Sciences,
Brighton & Sussex Medical School, University of Sussex,
Brighton, BN7 3PB, UK
e-mail: k.a.miles@bsms.ac.uk
Tel.: +44-0127-3877574

Keywords: Non-small cell lung cancer – Tumour blood flow – Glucose metabolism – Tumour size – ^{18}F-FDG

Eur J Nucl Med Mol Imaging (2006) 33:22–28
DOI 10.1007/s00259-005-1932-7

Introduction

Meta-analysis has confirmed positron emission tomography (PET) with ^{18}F-fluorodeoxyglucose (FDG) to be a highly accurate method for characterisation of pulmonary nodules [1]. More recently, perfusion-based imaging techniques such as quantitative contrast-enhanced computed tomography (CE-CT) have been advocated as an alternative means to characterise pulmonary nodules on the basis that angiogenesis within malignant nodules will be depicted as increased perfusion [2, 3]. Several studies have shown that measurements of contrast enhancement of lung tumours during CE-CT correlate with histological assessments of angiogenesis such as microvessel density, and with expression of vascular endothelial growth factor [4–6]. Incorporation of CE-CT into clinical pathways for the management of pulmonary nodules is also potentially cost-effective [7]. Furthermore, FDG-PET and perfusion imaging have both been proposed as methods for evaluating the response of lung and other tumours to therapy [8–11].

For FDG-PET and CE-CT to be considered equivalent methods for diagnosis and response evaluation of lung cancer, there would need to be a constant relationship between tumour glucose metabolism and perfusion. However, previous studies evaluating the relationship between blood flow and glucose metabolism in lung tumours have yielded variable results. Non-small cell lung cancers (NSCLCs) in

patients undergoing surgical resection have exhibited statistically significant correlations relating PET measurements of tumour glucose metabolism to perfusion imaging [12]. Yet no such correlations were found amongst patients with stage IIIA, N2 NSCLC or amongst patients with pulmonary metastases [13, 14]. In addition, variable changes in glucose metabolism and blood flow in response to treatment have been observed for a range of tumour types in which uncoupling of glucose metabolism and flow was found to be particularly likely after therapy targeting the tumour vasculature [15–18].

The above studies suggest a complex relationship between tumour metabolism and blood flow, with the possibility that blood flow and metabolism are coupled in early resectable NSCLC but may become uncoupled in the later stages of disease and following therapy. Furthermore, the precise relationship between blood flow and metabolism could provide a useful indicator of the biological behaviour of an individual tumour. Metabolism sufficient for tumour growth requires an adequate delivery of glucose and oxygen, for which a well-developed tumour vascular supply is essential. However, tumour glucose metabolism is also stimulated by hypoxia, which may occur when the tumour blood flow is inadequate [19, 20]. Tumour hypoxia is known to be associated with tumour aggression and a poor response to a variety of therapeutic strategies [19]. Hence, assessment of both tumour blood flow and glucose metabolism may provide a clearer picture of the biological characteristics of a tumour than either method alone. With the advent of integrated PET-CT systems, tumour flow–metabolic relationships could potentially be assessed by combining FDG-PET and CE-CT in a single examination.

Thus, the aim of this study was to undertake dual assessment of tumour blood flow and glucose metabolism in NSCLC using CE-CT and FDG-PET in order to assess how the relationships between these parameters vary with tumour size and stage.

Materials and methods

Patients

The study was undertaken as a sub-protocol that comprised all patients with NSCLC from a larger research program evaluating FDG uptake and CT contrast enhancement in a range of tumour types. This research program had been approved by the local ethics committee. Informed written consent was obtained in all patients. Seventeen patients with biopsy-proven NSCLC were recruited consecutively, comprising 11 men and 6 women with a mean age of 64 years. One patient had synchronous tumours, providing a total of 18 evaluable lesions.

All patients underwent FDG-PET and CE-CT as part of their clinical care, with quantitative CE-CT added to a conventional diagnostic CT. PET and CT examinations were performed within 48 h using separate imaging systems. As many patients did not undergo surgery, tumour stage was defined from the clinical reports of the findings on PET and conventional CT, evaluated together. Staging of NSCLC with PET in addition to CT has been shown to provide accurate prognostic stratification [21].

Positron emission tomography

A standard PET imaging technique was used. Following a 6-h fast, whole-body PET images were acquired 60 min after intravenous administration of 120–200 MBq FDG using a GE QUEST dedicated PET scanner (GE Medical Systems, Milwaukee, WI). Transmission scanning was performed and attenuation-corrected images (128×128 pixels, slice thickness of 4 mm) were produced by iterative reconstruction using the ordered subset expectation maximisation (OSEM) algorithm [22]. A transaxial slice at an anatomical level corresponding to the CE-CT study was selected for quantitative analysis. A region of interest (ROI) was drawn around the tumour by an operator

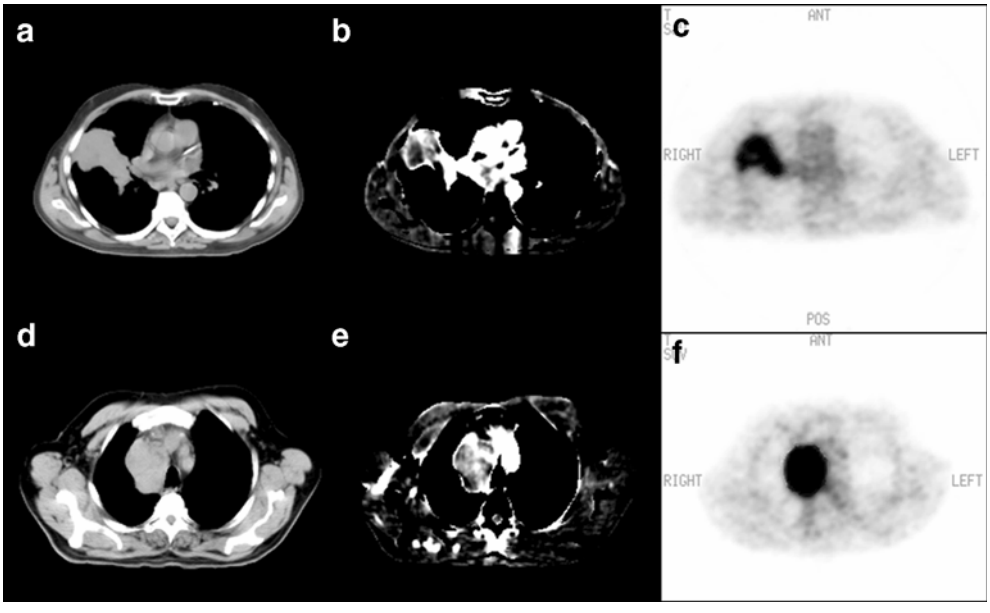

Fig. 1. Example conventional CT images (**a**,**d**), peak enhancement images (**b**,**e**) and FDG images (**c**,**f**). *Upper row*: stage II tumour of area 26.5 cm^2 with a metabolic–flow difference of 3.77. *Lower row*: stage IV tumour of area 28.1 cm^2 with a metabolic–flow difference of 7.65

Table 1. Summary of tumour types and measurements

Tumour	Pathology	Tumour area (cm^2)	Stage	SUV	SPV	SUV/SPV	Metabolic–flow difference
1	Adenocarcinoma	3.55	I	3.58	1.82	1.97	1.76
2	Adenocarcinoma	5.25	I	5.45	6.71	0.81	−1.26
3	Adenocarcinoma	0.65	I	7.54	5.79	1.30	1.75
4	Mucinous adenocarcinoma	3.30	I	2.8	1.51	1.85	1.29
5	Adenocarcinoma	1.44	II	4.78	1.48	3.23	3.30
6	Adenocarcinoma	26.15	II	6.35	2.58	2.47	3.77
7	Squamous cell	11.85	II	6.33	4.95	1.28	1.38
8	Squamous cell	6.55	II	7.83	1.64	4.77	6.19
9	Adenocarcinoma	12.16	III	6.44	1.34	4.79	5.10
10	Adenocarcinoma	32.98	III	9.12	1.55	5.89	7.57
11	Adenocarcinoma	3.61	III	6.26	2.98	2.10	3.28
12	Poorly differentiated adenocarcinoma	9.25	III	5.82	4.85	1.20	0.97
13	Poorly differentiated adenocarcinoma	5.05	III	7.39	6.52	1.13	0.87
14	Poorly differentiated adenocarcinoma	28.04	III	9.75	2.10	4.64	7.65
15	Adenocarcinoma	1.07	IV	5.54	4.40	1.26	1.14
16	Adenocarcinoma	42.12	IV	6.41	1.99	3.21	4.42
17	Adenocarcinoma	7.53	IV	7.86	3.31	2.38	4.55
18	Poorly differentiated carcinoma	19.30	IV	10.36	2.39	4.33	7.97

blinded both to the CE-CT results and to the final tumour stage. Using standard software installed on the PET system, the FDG uptake within the tumour was expressed as the standardised uptake value (SUV) calculated from:

$$SUV = \frac{Activity\ concentration\ (MBq/g)}{[Injected\ dose\ (MBq)/Patient\ weight\ (g)]} \quad (1)$$

CT image acquisition

Quantitative CE-CT was incorporated into the patients' conventional CT examination performed for clinical tumour staging. A single location dynamic sequence of images was acquired at the anatomical level containing the largest transverse dimension of the lung tumour. Fifty millilitres of conventional contrast material (Iopamidol, Bracco, Milan) with an iodine concentration of 370 mg/ml was administered intravenously at 7 ml/s. Patients were instructed to hold their breath during the 30-s examination. Data acquisition started at the time of contrast material injection, and ten images of 1 s duration with a slice thickness of 10 mm (120 kVp, 300 mAs) were obtained using a cycle time of 3 s. The CT images were exported for subsequent analysis by means of the digital imaging and communications in medicine (DICOM) protocol.

CT image analysis

Analysis of CE-CT studies was performed using Winfun software (Cambridge Computed Imaging, Bourne, UK). The operator was unaware of the PET findings at the time of the analysis. ROIs encompassing each tumour were created from the pre-contrast CT image displayed with a constant window width and level (300 HU and 0 HU respectively). This initial tumour ROI was refined using an automated method that removed pixels containing air or calcium by only retaining pixels with initial attenuation values between −50 HU and 100 HU. Large blood vessels were also excluded from the ROI by eliminating pixels that enhanced by more than 100 HU following contrast material injection. The area of the final ROI was recorded as a measure of tumour size that avoided the errors associated with manual measurements [23].

The changes in the x-ray attenuation within the tumour ROI following administration of contrast material were displayed as a time–attenuation curve. The first image prior to administration of contrast material was subtracted from the image in which the attenuation within tumour ROI was maximal, thereby generating a parametric image displaying peak tumour enhancement (Fig. 1). The peak enhancement of the whole tumour was recorded. To allow direct

Table 2. Regression analysis relating tumour area to SUV from FDG-PET and SPV from CT

	No.	Correlation coefficient (r)	Slope (95% CI)	p value
Standardised uptake value (SUV)	18	0.47	0.75 (0.001–1.49)	0.046[a]
Standardised perfusion value (SPV)	18	0.42	−0.39 (−0.84–0.6)	0.083
Ratio of SUV to SPV	18	*0.56*	*0.072 (0.016–0.127)*	*0.015*
Metabolic–flow difference	18	*0.60*	*0.13 (0.04–0.22)*	*0.008*

Statistically significant results are in italics

CI confidence limits

[a]Not statistically significant with Bonferroni correction.

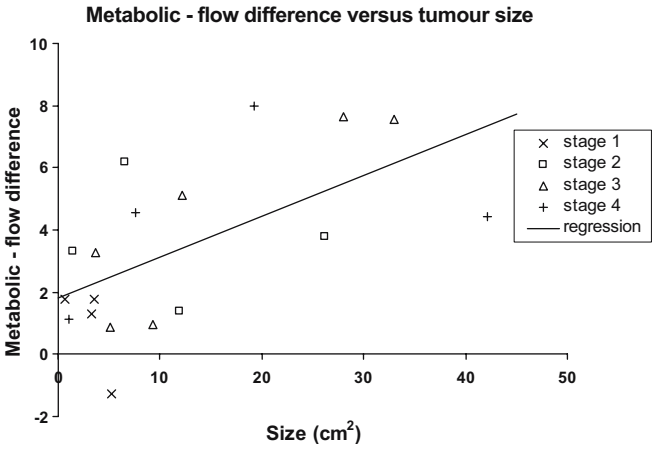

Fig. 2. Relationship between metabolic–flow difference and tumour size

comparison with SUV measurements on PET, the peak enhancement value was converted to concentration of iodine and normalised for injected dose of contrast material and patient weight, as described previously, the resulting value reflecting blood flow expressed as the standardised perfusion value (SPV) [24]. Calculation of SPV is directly analogous to the calculation of SUV, as shown by:

$$SPV = \frac{Peak\ \ iodine\ \ concentration\ \ (mgI/g)}{[Dose\ \ (mgI)/Patient\ \ weight\ \ (g)]} \quad (2)$$

Combined measures of blood flow and metabolism

The relationship between blood flow and metabolism was expressed as the ratio of SUV to SPV and as the metabolic–flow difference defined by [SUV–SPV]. SPV and SUV have equivalent derivations, reflecting respectively the delivery of plasma to the tumour and uptake of FDG into the tumour.

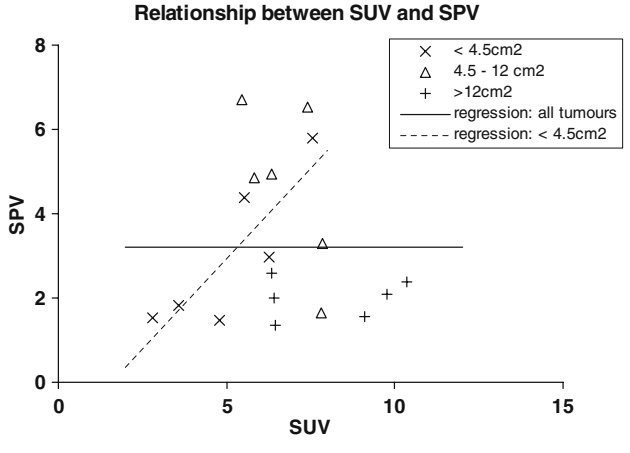

Fig. 3. Tumour SPV plotted against SUV. There is no correlation amongst all tumours (*solid line*) but a significant correlation for tumours less than 4.5 cm^2 (*dotted line*)

Statistical analysis

The dependence of FDG uptake and contrast enhancement on tumour size was explored by performing regression analysis of size against SUV, SPV and combined parameters. For this multivariate analysis, the Bonferroni correction was applied, such that a p value of 0.015 or less would indicate statistical significance. Tumours were also divided into three groups separated by the 33rd and 67th percentiles (tertiles) for tumour size. Regression analysis was performed to evaluate the relationship between SUV and SPV amongst all tumours and within each group separately using a p value of 0.05 for statistical significance.

Results

The mean (range) tumour size was 12.2 (0.65–42.1) cm^2. Six tumours were stage III NSCLCs whilst stages I, II and IV comprised four tumours each. Table 1 summarises the individual tumour types and measurements. Table 2 displays the results of regression analysis relating tumour area to SUV, SPV and combined parameters. Allowing for the Bonferroni correction, no significant correlation was found between tumour size and SUV or SPV. However, the ratio of SUV to SVP and the metabolic–flow difference did correlate with tumour size, with higher values found in larger tumours (Fig. 2). A metabolic–flow difference of greater than 4 was found in six of ten tumours of stages III and IV but in only one of eight tumours of stages I and II (odds ratio 10.5; 95% confidence limits 0.24–32.1). This finding is illustrated by the examples in Fig. 1, in which the two tumours are of similar size but the stage IV tumour demonstrates a higher metabolic–flow difference.

There was no significant correlation between SUV and SPV for all tumours (r=0.0, p=0.99, Fig. 3). However, when the tumours were divided into three equal groups using upper and lower tertile values for size (4.5 and 12.0 cm^2 respectively), a significant correlation between SUV and SPV was found for tumours smaller than 4.5 cm^2 (r=0.85, p<0.05, Table 3).

Table 3. Relationship between SUV for FDG and SPV: effect of tumour size

	No.	Correlation coefficient (r)	Slope (95% CI)	p value
All tumours	18	0.0	0.0 (−0.50–0.50)	0.99
Tumour area <4.5 cm^2	6	*0.85*	*0.86 (0.12–1.6)*	*0.03*
Tumour area 4.5–12.0 cm^2	6	0.64	−1.18 (−3.14–0.78)	0.17
Tumour area >12 cm^2	6	0.15	0.04 (−0.31–0.39)	0.77

Statistically significant results are in italics
CI confidence limits

Discussion

Our findings indicate that the relationship between tumour blood flow and glucose metabolism in NSCLC is dependent upon tumour size, with the greatest metabolic–flow differences found in larger tumours of higher stage. This variability in blood flow–metabolic relationships indicates that FDG-PET and quantitative CE-CT cannot be considered equivalent markers of malignancy. The finding of low perfusion in large tumours highlights an important pitfall for quantitative CE-CT in the diagnostic assessment of pulmonary nodules, particularly for nodules with a diameter greater than approximately 2.5 cm. Histological studies in lung carcinomas have shown that this pitfall is likely to be due to an association between tumour necrosis and lower contrast enhancement [25].

The dependence of blood flow–metabolic relationships on tumour size and stage also offers an explanation for the disparate results of previous studies. The previous study reporting a correlation between FDG uptake and perfusion-based measures on CT comprised patients with NSCLC suitable for surgical resection and with a mean tumour diameter of 2.9±0.3 cm [12]. Our data indicate that a similar correlation exists for tumours of a similar size, i.e. with an area of less than 4.5 cm^2, equivalent to a mean diameter of 2.4 cm. However, our results indicate a trend for blood flow to be lower in larger tumours, with all tumours over 12 cm^2 (equivalent to a mean diameter of 3.9 cm) having an SPV of 2.85 or less. This finding is in keeping with the results of Kiessling et al., who reported lower CT perfusion values in bronchial carcinomas with a volume greater than 50 cm^3 (equivalent to a mean diameter of 4.6 cm) [11]. For glucose metabolism, we found an opposite trend, with greater FDG uptake in larger tumours, such that the metabolic–flow difference correlated with tumour size, implying uncoupling of blood flow and glucose metabolism in larger tumours. Such uncoupling could explain the lack of correlation between tumour blood flow and metabolism found in the previous study of stage IIIA NSCLC [13]. Although tumour sizes were not reported in that series, the study probably would have included larger tumours in view of the advanced stage. A greater degree of uncoupling, as seen in high stage tumours in our series, might also be expected amongst pulmonary metastases, as found previously [14].

The finding of a trend towards greater metabolic–flow differences in tumours of advanced stage suggests that the relationship between blood flow and metabolism could provide an indicator of biological behaviour for individual tumours. In lung cancer, elevated glucose metabolism and high levels of angiogenesis are both associated with increased metastatic potential and poor patient survival [26–33]. However, as tumours increase in size, they may outgrow their blood supply. The subsequent reduction in the delivery of oxygen renders such tumours hypoxic [20]. Tumours can adapt to hypoxia by increasing expression of glucose transporters and by utilising anaerobic glycolysis, a process mediated by hypoxia-inducible factors (HIF) [19, 20]. Hypoxia also induces an aggressive tumour phenotype that is resistant to therapy [19], and increased expression of HIF in NSCLC with low microvessel density is associated with a worse prognosis [34]. The results of our imaging studies reflect these aspects of tumour molecular biology in that NSCLCs with a high metabolic–flow difference were more likely to be tumours of high stage.

Imaging of tumour hypoxia is increasingly an issue of clinical importance, not only in the context of resistance to therapy but also with the emergence of chemotherapeutic agents, such as tirapazamine, and gene therapy strategies that target hypoxia [19]. Imaging studies that use PET tracers, such as fluoromisonidazole (F-MISO), for which uptake is proportional to tissue hypoxia, have demonstrated that hypoxia is a common finding in NSCLC [35]. Although reflecting tumour hypoxia, uptake of F-MISO provides no information about the ability of tumour cells to adapt to hypoxia, for example by increasing glycolysis. Indeed, studies have shown discordance between uptake of F-MISO and FDG in a range of tumours [36, 37]. The association between low perfusion and tumour hypoxia suggests that CE-CT can provide an alternative imaging marker of hypoxia which could be combined in a single examination with FDG-PET studies performed on integrated PET-CT systems. Integrated PET-CT is increasingly used for staging of lung cancer in clinical practice, but to date the CT component of combined PET-CT examinations has generally comprised an examination without contrast medium, primarily for attenuation correction and anatomical assignment of abnormalities identified on PET [38]. However, there is growing interest in the use of intravenous contrast media during PET-CT [39]. The ability to quantify contrast enhancement in terms of tissue perfusion was demonstrated on clinical CT systems in the early 1990s [40], and experience of quantitative CE-CT on stand-alone CT systems has shown that the perfusion data can be easily obtained as part of a conventional contrast enhancement protocol [41]. Such techniques would be readily transferable to integrated PET systems and so provide, in a single examination, conventional PET-CT imaging as well as metabolic–flow data of potential value in characterising aspects of tumour biology indicative of tumour aggression and likely response to therapy.

In summary, blood flow–metabolic relationships are not consistent in NSCLC but are dependent upon tumour size and stage. Quantitative CE-CT as an adjunct to an FDG study undertaken using integrated PET-CT offers an efficient way to augment the assessment of tumour biology with possible future application as part of clinical care.

Acknowledgements. This study was supported by a grant from the Wesley Research Institute (WRI), Brisbane, Australia. WRI had no involvement in study design; collection, analysis, and interpretation of data; writing of the report, nor in the decision to submit the paper for publication.

References

1. Gould MK, Maclean CC, Kuschner WG, Rydzak CE, Owens DK. Accuracy of positron emission tomography for diagnosis of pulmonary nodules and mass lesions: a meta-analysis. JAMA 2001;285:914–24
2. Swensen SJ, Viggiano RW, Midthun DE, Muller NL, Sherrick A, Yamashita K, et al. Lung nodule enhancement at CT: multicenter study. Radiology 2000;214:73–80
3. Pastorino U, Bellomi M, Landoni C, De Fiori E, Arnaldi P, Picchio M, et al. Early lung-cancer detection with spiral CT and positron emission tomography in heavy smokers: 2-year results. Lancet 2003;362:593–7
4. Swensen SJ, Brown LR, Colby TV, Weaver AL, Midthun DE. Lung nodule enhancement at CT: prospective findings. Radiology 1996;201:447–55
5. Tateishi U, Nishihara H, Watanabe S, Morikawa T, Abe K, Miyasaka K. Tumor angiogenesis and dynamic CT in lung adenocarcinoma: radiologic-pathologic correlation. J Comput Assist Tomogr 2001;25:23–7
6. Yi CA, Lee KS, Kim EA, Han J, Kim H, Kwon OJ, et al. Solitary pulmonary nodules: dynamic enhanced multi-detector row CT study and comparison with vascular endothelial growth factor and microvessel density. Radiology 2004;233:191–9
7. Comber LA, Keith CJ, Griffiths M, Miles KA. Solitary pulmonary nodules: impact of quantitative contrast-enhanced CT on the cost-effectiveness of FDG-PET. Clin Radiol 2003;58: 706–11
8. Young H, Baum R, Cremerius U, Herholz K, Hoekstra O, Lammertsma AA, et al. Measurement of clinical and subclinical tumour response using [^{18}F]-fluorodeoxyglucose and positron emission tomography: review and 1999 EORTC recommendations. European Organization for Research and Treatment of Cancer (EORTC) PET Study Group. Eur J Cancer 1999;35: 1773–82
9. Mac Manus MP, Hicks R J, Matthews JP, McKenzie A, Rischin D, Salminen EK, et al. Positron emission tomography is superior to computed tomography scanning for response-assessment after radical radiotherapy or chemoradiotherapy in patients with non-small-cell lung cancer. J Clin Oncol 2003;21:1285–92
10. Miller JC, Pien HH, Sahani D, Sorensen G, Thrall JH. Imaging angiogenesis: applications and potential for drug development. J Natl Cancer Inst 2005;97:172–87
11. Kiessling F, Boese J, Corvinus C, Ederle JR, Zuna I, Schoenberg SO, et al. Perfusion CT in patients with advanced bronchial carcinomas: a novel chance for characterization and treatment monitoring? Eur Radiol 2004;14:1226–33
12. Tateishi U, Nishihara H, Tsukamoto E, Morikawa T, Tamaki N, Miyasaka K. Lung tumors evaluated with FDG-PET and dynamic CT: the relationship between vascular density and glucose metabolism. J Comput Assist Tomogr 2002;26:185–90
13. Hoekstra CJ, Stroobants SG, Hoekstra OS, Smit EF, Vansteenkiste JF, Lammertsma AA. Measurement of perfusion in stage IIIA-N2 non-small cell lung cancer using $H_2{}^{15}O$ and positron emission tomography. Clin Cancer Res 2002;8:2109–15
14. Veronesi G, Landoni C, Pelosi G, Picchio M, Sonzogni A, Leon ME, et al. Fluoro-deoxi-glucose uptake and angiogenesis are independent biological features in lung metastases. Br J Cancer 2002;86:1391–5
15. Mullani N, Herbst R, Abbruzzese J, Charnsangavej C, Kim E, Tran H, et al. Antiangiogenic treatment with endostatin results in uncoupling of blood flow and glucose metabolism in human tumors. Clin Positron Imaging 2000;3:151
16. Mankoff DA, Dunnwald LK, Gralow JR, Ellis GK, Schubert EK, Tseng J, et al. Changes in blood flow and metabolism in locally advanced breast cancer treated with neoadjuvant chemotherapy. J Nucl Med 2003;44:1806–14
17. Kurdziel KA, Figg WD, Carrasquillo JA, Huebsch S, Whatley M, Sellers D, et al. Using positron emission tomography 2-deoxy-2-[^{18}F]fluoro-D-glucose, ^{11}CO, and ^{15}O-water for monitoring androgen independent prostate cancer. Mol Imaging Biol 2003;5:86–93
18. Willett CG, Boucher Y, di Tomaso E, Duda DG, Munn LL, Tong RT, et al. Direct evidence that the VEGF-specific antibody bevacizumab has antivascular effects in human rectal cancer. Nat Med 2004;10:145–7
19. Semenza GL. HIF-1 and tumor progression: pathophysiology and therapeutics. Trends Mol Med 2002;8 4 Suppl:S62–7
20. Raghunand N, Gatenby RA, Gillies RJ. Microenvironmental and cellular consequences of altered blood flow in tumours. Br J Radiol 2003;76:11–22
21. Hicks RJ, Kalff V, MacManus MP, Ware RE, Hogg A, McKenzie AF, et al. ^{18}F-FDG PET provides high-impact and powerful prognostic stratification in staging newly diagnosed non-small cell lung cancer. J Nucl Med 2001;42:1596–604
22. Benard F, Smith RJ, Hustinx R, Karp JS, Alavi A. Clinical evaluation of processing techniques for attenuation correction with Cs-137 in whole body PET imaging. J Nucl Med 1999; 40:1257–63
23. Erasmus JJ, Gladish GW, Broemeling L, Sabloff BS, Truong MT, Herbst RS, et al. Interobserver and intraobserver variability in measurement of non-small-cell carcinoma lung lesions: implications for assessment of tumor response. J Clin Oncol 2003;21:2574–82
24. Miles KA, Griffiths MR, Fuentes MA. Standardized perfusion value: universal CT contrast enhancement scale that correlates with FDG PET in lung nodules. Radiology 2001;220:548–53
25. Yamashita K, Matsunobe S, Tsuda T, Okuda K, Matsumoto K, Oyanagi H, et al. Intratumoral necrosis of lung carcinoma: a potential diagnostic pitfall in incremental dynamic computed tomography analysis of solitary pulmonary nodules? J Thorac Imaging 1997;12:181–7
26. Ahuja V, Coleman RE, Herndon J, Patz EF Jr. The prognostic significance of fluorodeoxyglucose positron emission tomography imaging for patients with nonsmall cell lung carcinoma. Cancer 1998;83:918–24
27. Vansteenkiste JF, Stroobants SG, Dupont PJ, De Leyn PR, Verbeken EK, Deneffe GJ, et al. Prognostic importance of the standardized uptake value on ^{18}F-fluoro-2-deoxy-glucose-positron emission tomography scan in non-small-cell lung cancer: an analysis of 125 cases. Leuven Lung Cancer Group. J Clin Oncol 1999;17:3201–6
28. Higashi K, Ueda Y, Arisaka Y, Sakuma T, Nambu Y, Oguchi M, et al. ^{18}F-FDG uptake as a biologic prognostic factor for recurrence in patients with surgically resected non-small cell lung cancer. J Nucl Med 2002;43:39–45
29. Jeong HJ, Min JJ, Park JM, Chung JK, Kim BT, Jeong JM, et al. Determination of the prognostic value of [^{18}F] fluorodeoxyglucose uptake by using positron emission tomography in patients with non-small cell lung cancer. Nucl Med Commun 2002;23:865–70
30. Downey RJ, Akhurst T, Gonen M, Vincent A, Bains MS, Larson S, et al. Preoperative F-18 fluorodeoxyglucose-positron emission tomography maximal standardized uptake value predicts survival after lung cancer resection. J Clin Oncol 2004; 22:3255–60

31. Fontanini G, Bigini D, Vignati S, Basolo F, Mussi A, Lucchi M, et al. Microvessel count predicts metastatic disease and survival in non-small cell lung cancer. J Pathol 1995;177:57–63
32. Meert AP, Paesmans M, Martin B, Delmotte P, Berghmans T, Verdebout JM, et al. The role of microvessel density on the survival of patients with lung cancer: a systematic review of the literature with meta-analysis. Br J Cancer 2002;87:694–701
33. Tanaka F, Yanagihara K, Otake Y, Kawano Y, Miyahara R, Takenaka K, et al. Prognostic factors in resected pathologic (p-) stage IIIA-N2, non-small-cell lung cancer. Ann Surg Oncol 2004;11:612–8
34. Giatromanolaki A, Koukourakis MI, Sivridis E, Turley H, Talks K, Pezzella F, et al. Relation of hypoxia inducible factor 1 alpha and 2 alpha in operable non-small cell lung cancer to angiogenic/molecular profile of tumours and survival. Br J Cancer 2001;85:881–90
35. Foo SS, Abbott DF, Lawrentschuk N, Scott AM. Functional imaging of intratumoral hypoxia. Mol Imaging Biol 2004;6: 291–305
36. Rajendran JG, Wilson DC, Conrad EU, Peterson LM, Bruckner JD, Rasey JS, et al. [^{18}F]FMISO and [^{18}F]FDG PET imaging in soft tissue sarcomas: correlation of hypoxia, metabolism and VEGF expression. Eur J Nucl Med Mol Imaging 2003;30:695–704
37. Rajendran JG, Mankoff DA, O'Sullivan F, Peterson LM, Schwartz DL, Conrad EU, et al. Hypoxia and glucose metabolism in malignant tumors: evaluation by [^{18}F]fluoromisonidazole and [^{18}F]fluorodeoxyglucose positron emission tomography imaging. Clin Cancer Res 2004;10:2245–52
38. Lardinois D, Weder W, Hany TF, Kamel EM, Korom S, Seifert B, et al. Staging of non-small-cell lung cancer with integrated positron-emission tomography and computed tomography. N Engl J Med 2003;348:2500–7
39. Antoch G, Freudenberg LS, Beyer T, Bockisch A, Debatin JF. To enhance or not to enhance? ^{18}F-FDG and CT contrast agents in dual-modality ^{18}F-FDG PET/CT. J Nucl Med 2004;45:56S–65S
40. Miles KA, Hayball MP, Dixon AK. Colour perfusion imaging: a new application of computed tomography. Lancet 1991;337: 643–5
41. Miles KA, Griffiths MR. Perfusion CT: a worthwhile enhancement? Br J Radiol 2003;76:220–31